Monte Carlo simulation of asymmetrical growth of cube-shaped nanoparticles*

Yuanyuan Wang(王元元), Huaqing Xie(谢华清)†, Zihua Wu(吴子华), and Jiaojiao Xing(邢姣娇)

School of Environmental and Materials Engineering, Shanghai Polytechnic University, Shanghai 201209, *China*

(Received 24 March 2016; revised manuscript received 17 May 2016; published online 19 July 2016)

We simulated the asymmetrical growth of cube-shaped nanoparticles by applying the Monte Carlo method. The influence of the specific mechanisms on the crystal growth of nanoparticles has been phenomenologically described by efficient growth possibilities along different directions (or crystal faces). The roles of the thermodynamic and kinetic factors have been evaluated in three phenomenological models. The simulation results would benefit the understanding about the cause and manner of the asymmetrical growth of nanoparticles.

Keywords: cube-shaped nanoparticles, asymmetrical growth, Monte Carlo simulation

PACS: 61.46.Fg, 61.46.Km, 61.43.Bn **DOI:** 10.1088/1674-1056/25/9/096104

1. Introduction

Shape control of metal nanostructures is a promising strategy of tailoring their physical, chemical, and biocompatible properties for various applications, such as catalysis, sensing, bioimaging, photothermal therapy, plasmonics, and spectroscopy.[1–4] Most metals crystallize in the same cubic close-packed structure: a face-centered cubic (fcc) lattice. It is known that the external morphology of a crystal is decided by its internal point group symmetry. During the past decade, a wide variety of polyhedral fcc metal (gold, silver, etc.) nanostructures with O_h symmetry, including cubes, truncated cubes, cuboctahedra, truncated octahedra, and octahedra, have been synthesized.[2,4,5] These cases are consistent with the point group symmetry of the crystals. In the meantime, highly anisotropic metal nanostructures which do not conserve the point group symmetry were also widely reported in the literature, for example, one dimensional (1D) rods and wires.[6,7] This raises the critical issue here: why and how asymmetrical growths could take place in the fcc metals? As we know, there are several mechanisms that could lead to asymmetrical growth of the fcc crystals. Commonly, twinning has been proven as a cause of asymmetrical growth of metals and produces multiple twinned particles.[2] Shen *et al.* demonstrated an alternative mechanism for the formation of 1D silver nanostructures, in which continuous formation of (111) twins, local 4H phase, and other stacking faults along one direction induces the asymmetrical growth of the crystal of fcc silver.[8] In the case of two-dimensional nanoplate,[9] twinning also plays an important role, though the detail has not yet been revealed. Moreover, oriented attachment is another important mechanism of the formation of 1D nanostructure that involves a spontaneous self-organization of adjacent particles.[10,11] Differing from the above mentioned mechanisms, the evolution of a single-crystal nanoparticle, e.g. a nanocube, to a 1D nanostructure is mysterious and unexplored. Obviously, this evolution is a kinetic-controlled growth. A kinetic-controlled growth here refers to a growth leading to some shapes which deviate from the thermodynamic equilibrium one with minimal Gibbs free energy. In fcc materials, the surface energies γ of low-index crystallographic facets have the energetic sequence of $\gamma\{111\} < \gamma\{100\} < \gamma\{110\}$.[12] As a result, the equilibrium shape is the truncated octahedron (or Wulff polyhedron) for the single-crystal fcc nanoparticles. However, the preferential binding of additives to certain crystal facets can alter the sequence of the surface energies, and thus other shapes, like the cube enclosed by six $\{100\}$ facets, may become the equilibrium one. As an example, bromide binds most strongly to the $\{100\}$ facets of Ag, Pd, and Pt. This benefits the formation of nanocubes.[2,4,13–15]

A cube has a smaller surface area than a cuboid of the same volume, which means a lower Gibbs free energy. However, we find exceptions in almost every case, where considerable numbers of cuboid nanoparticles exist among the cubic particle clusters, especially when the average size of the particles is smaller than 10 nm. The aspect ratio r between the longest side $l_{\max}$ and the shortest side $l_{\min}$ of these cuboid nanoparticles is usually smaller than 1.5. This phenomenon appears in metals,[13–16] alloys,[17,18] and even metallic oxides.[19,20] Besides the microcubes assembled by Pd nanocubes, some cuboid microstructures can also be obtained. All these experimental results indicate that this asymmetrical growth may not arise from some specific

*Project supported by the National Natural Science Foundation of China (Grant No. 51406111), the Major Program of the National Natural Science Foundation of China (Grant No. 51590902), the Natural Science Foundation of Shanghai, China (Grant No. 14ZR1417000), the Scientific Innovation Project of Shanghai Education Committee, China (Grant No. 15ZZ100), and Young Eastern Scholar of Shanghai, China (Grant No. QD2015052).

†Corresponding author. E-mail: hqxie@sspu.edu.cn

© 2016 Chinese Physical Society and IOP Publishing Ltd

kinetic mechanisms, but from thermodynamics alone. For a nanocube, the three directions are equivalent under the thermodynamics-controlled growth. Therefore, the formation of cuboid nanoparticles must be governed by extra mechanisms, which means that the growth is preferable along one direction rather than equally along three directions. So far, several kinetic mechanisms, such as surfactant-assisted growth,[4,21] electric-field-directed growth,[22] and localized-oxidative-etching-promoted growth,[23] have been proposed to account for the formation of 1D nanostructures whose aspect ratios are usually larger than 2. Although some asymmetrical growth mechanisms have been proposed.[24] for cases like the experimental results, there are very limited theoretical works that can be used to quantitatively understand the observations. To explore the asymmetrical growth mechanism of cube-shaped nanoparticles, we establish models to study the role of thermodynamic and kinetic factors in the anisotropic growth of cube-shaped nanoparticles using Monte Carlo (MC) simulation.

2. Model

The growth of a nanoparticle can be described by the growth rate along specific faces or directions. In consideration that the synthesis of the cube-shaped nanoparticles often takes place in the solutions, the growth of the particles is not limited by the substrate. When the particles are crowded, the side facing a neighbor particle will have reduced chance to grow. However, it is acceptable to neglect this neighborhood competition when the concentration of the particles is low.

We focus on why and how the cuboids appear among cubes. We can simplify the cube formation simulation using a simple cubic (sc) model instead of the fcc model. In a homopolar crystal with a simple cubic lattice, each atom can be treated as a cube. Because bonding may occur at each face of the cube, an atom may have up to six first-nearest neighbors. The interactions of the particle with its second and third neighbors, which share an edge and corners with the particle, respectively, also exist. However, the interactions with the second and the third neighbors are much weaker than that with the first-nearest neighbors and therefore can be neglected reasonably. In the beginning of the crystallization, hundreds of atoms assemble under the nucleation mechanism. To simplify, this atom assembly is assumed to be a cube. A new atom attaches on one of the six faces of the cube with equal possibility. Then another atom tends to attach on the already formed assembly at the site where most chemical bonding can be formed, which means that the attachment process favors releasing the maximum energy. Therefore, if an atom attaches on one face, a whole layer including that atom is formed soon after being adhered to that face. Another layer is then formed, and so on. This is the well-known layer growth model (Kossel–Stranski model).[25–27] Our simulation is based on the layer growth model. The schematic figure of the growth process is shown in Fig. 1. There is no harm to the universality assuming the width of each unit cube, representing an atom, is 1. The seeding nuclei are set to be $5\times5\times5$ cubes, representing clusters containing 125 atoms. There are two growth factors which affect the growth of the nanoparticle. One is the thermodynamic factor and the other is the kinetic factor. Assuming growth directions of the cube are along the x, y, and z axes, with the normalization condition considered, we can write down a general expression of the growth possibilities as

$$\boldsymbol{P}=(1-\gamma)\frac{\boldsymbol{F}^{\mathrm{t}}}{|\boldsymbol{F}^{\mathrm{t}}|}+\gamma\frac{\boldsymbol{F}^{\mathrm{k}}}{|\boldsymbol{F}^{\mathrm{k}}|}, \tag{1}$$

where $\boldsymbol{P}\equiv(P_x,P_y,P_z)^{\mathrm{T}}$, $\boldsymbol{F}^{\mathrm{t}}\equiv\left(F_x^{\mathrm{t}},F_y^{\mathrm{t}},F_z^{\mathrm{t}}\right)^{\mathrm{T}}$ and $\boldsymbol{F}^{\mathrm{k}}\equiv\left(F_x^{\mathrm{k}},F_y^{\mathrm{k}},F_z^{\mathrm{k}}\right)^{\mathrm{T}}$ are the thermodynamics and kinetic terms, respectively, and their corresponding coefficients are $1-\gamma$ and γ. $\boldsymbol{F}^{\mathrm{t}}$ and $\boldsymbol{F}^{\mathrm{k}}$ are both functions of the cuboid particle size $\boldsymbol{l}$, where $\boldsymbol{l}\equiv(l_x,l_y,l_z)^{\mathrm{T}}$ and l_x, l_y, l_z stand for the side lengths along the x, y, z axes, respectively. $\boldsymbol{F}^{\mathrm{k}}$ and $\boldsymbol{F}^{\mathrm{t}}$ are then expanded in the basis of $\left\{l,l^2,l^3,\ldots\right\}$. Thus one obtains

$$\begin{aligned}\boldsymbol{F}^{\mathrm{t,k}}&=\begin{bmatrix}c_{0,x}^{\mathrm{t,k}}\\ c_{0,y}^{\mathrm{t,k}}\\ c_{0,z}^{\mathrm{t,k}}\end{bmatrix}+\begin{bmatrix}c_{1,xx}^{\mathrm{t,k}} & c_{1,xy}^{\mathrm{t,k}} & c_{1,xz}^{\mathrm{t,k}}\\ c_{1,yx}^{\mathrm{t,k}} & c_{1,yy}^{\mathrm{t,k}} & c_{1,yz}^{\mathrm{t,k}}\\ c_{1,zx}^{\mathrm{t,k}} & c_{1,zy}^{\mathrm{t,k}} & c_{1,zz}^{\mathrm{t,k}}\end{bmatrix}\begin{bmatrix}l_x\\ l_y\\ l_z\end{bmatrix}\\&+\begin{bmatrix}c_{2,x,xx}^{\mathrm{t,k}} & c_{2,x,yy}^{\mathrm{t,k}} & c_{2,x,zz}^{\mathrm{t,k}} & c_{2,x,yz}^{\mathrm{t,k}} & c_{2,x,zx}^{\mathrm{t,k}} & c_{2,x,xy}^{\mathrm{t,k}}\\ c_{2,y,xx}^{\mathrm{t,k}} & c_{2,y,yy}^{\mathrm{t,k}} & c_{2,y,zz}^{\mathrm{t,k}} & c_{2,y,yz}^{\mathrm{t,k}} & c_{2,y,zx}^{\mathrm{t,k}} & c_{2,y,xy}^{\mathrm{t,k}}\\ c_{2,z,xx}^{\mathrm{t,k}} & c_{2,z,yy}^{\mathrm{t,k}} & c_{2,z,zz}^{\mathrm{t,k}} & c_{2,z,yz}^{\mathrm{t,k}} & c_{2,z,zx}^{\mathrm{t,k}} & c_{2,z,xy}^{\mathrm{t,k}}\end{bmatrix}\begin{bmatrix}l_x^2\\ l_y^2\\ l_z^2\\ S_x\\ S_y\\ S_z\end{bmatrix}\\&+\cdots,\end{aligned} \tag{2}$$

where $\boldsymbol{c}_j$ $(j=1,2,3,\ldots)$ is the parameter of the j-th order term, $S_i=\varepsilon_{ijk}l_jl_k$ are the face areas perpendicular to the x, y, and z axes, respectively, and ε_{ijk} denotes the Levi–Civita tensor.

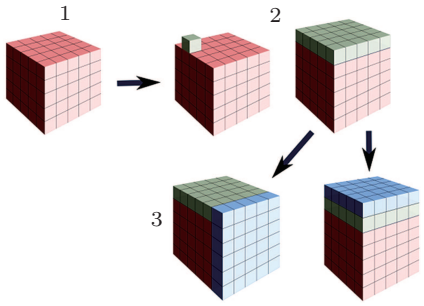


Fig. 1. Schematic of the layer growth model. Step 1: A small cube with size $5\times5\times5$ is introduced to represent a crystal nucleus. Step 2: A new layer is formed randomly on one of the six faces with equivalent possibilities since they are identical. Step 3: A new layer may attach on two different types of faces developed from step 2. Two sorts of cubes are formed.

2.1. Model with pure thermodynamics factor

First, we consider the growth process of the cuboid nanoparticle dominated only by the thermodynamic factor, which is isotropic. This model represents approximately the growth condition without anisotropic perturbations, like surfactant, nonuniform electric field, localized-oxidative-etching, and so on. After the nucleation process, many atoms move freely and perform random Brownian motion in the solution. The possibility that one atom attaches on a face is proportional to the area of that face, which means the growth possibility $P_i \propto S_i$ $(i = x, y, z)$. The thermodynamics term $\boldsymbol{F}^{\mathrm{t}}$ can be written as

$$\boldsymbol{F}^{\mathrm{t}} = \begin{bmatrix} 0 & 0 & 0 & 1 & 0 & 0 \\ 0 & 0 & 0 & 0 & 1 & 0 \\ 0 & 0 & 0 & 0 & 0 & 1 \end{bmatrix} \begin{bmatrix} l_x^2 \\ l_y^2 \\ l_z^2 \\ S_x \\ S_y \\ S_z \end{bmatrix}. \tag{3}$$

Since the kinetic factor is excluded, the kinetic term $\boldsymbol{F}^{\mathrm{k}} = 0$. Thus, equation (3) becomes

$$\boldsymbol{P} = \frac{\boldsymbol{S}}{S_{\mathrm{a}}}, \tag{4}$$

where $S_{\mathrm{a}} = \sum_{i=x,y,z} S_i$. In consideration of the isotropic property of the thermodynamic term, one can imagine that the particle should become a cube if its size is large enough ($l_i \gg 1$). When this condition has not been satisfied, the deviated degree of the particle from a cube should be studied numerically.

2.2. Model with both thermodynamic and shape-dependent kinetic factors

Then we consider the case with both thermodynamic and kinetic factors. Although several kinetic mechanisms, such as surfactant-assisted growth, electric-field-directed growth, and localized-oxidative-etching-promoted growth, have been proposed for certain types of inhomogeneous nanoparticle synthesis procedures respectively, we will focus on the common factor of these mechanisms to universally describe the effect of the kinetic factor. At the same time, the thermodynamic factor always exists and cannot be neglected.

One type of kinetic factor depends on the shape of the nanopaticle. Juste *et al.* attributed the inhomogeneous growth of gold nanorods to the electric field.[22] The nonuniform electric field is much larger at the tip of the nanorods than at the sides, and it gradually increases with the growth of the particles. This type of kinetic factor is a positive feedback process, which accelerates the inhomogeneous growth and lengthens the particle persistently along one direction once the asymmetrical growth takes place along this direction. To describe this type of kinetic factor, we consider that growth possibility P_i $(i = x, y, z)$ increases with l_i, which means increased growth possibility along the long side. The expression of the kinetic term in Eq. (3) can be given as

$$\boldsymbol{F}^{\mathrm{k}} = \begin{bmatrix} 1 & 0 & 0 \\ 0 & 1 & 0 \\ 0 & 0 & 1 \end{bmatrix} \begin{bmatrix} l_x \\ l_y \\ l_z \end{bmatrix}. \tag{5}$$

The thermodynamic term is the same as that in the previous model. Equation (3) is then deduced as

$$P = (1-\gamma)\,\boldsymbol{S}/S_{\mathrm{a}} + \gamma \boldsymbol{l}/l_{\mathrm{a}}, \tag{6}$$

where $l_{\mathrm{a}} = \sum_{i=x,y,z} l_i$ and γ represents the strength of the kinetic term. $0 \le \gamma \le 1$ should be satisfied to assure that the growth possibilities make sense. It is noticed that when $\gamma = 0$, this model returns to the previous model in Subsection 2.1, in which only the thermodynamic term is considered. We have analyzed in the previous subsection that at this time, the nanoparticle should become cube-shaped when its size is large enough. When $\gamma = 1$, this model only contains the kinetic term. As in our previous discussion, once the asymmetrical growth takes place along one direction, the kinetic term gives a positive feedback mechanism and continuously lengthens the nanoparticle along this direction. When $0 < \gamma < 1$, the thermodynamic and the kinetic factors induce opposite and competitive growth trends.

2.3. Model with both thermodynamic and shape-independent kinetic factors

In the previous subsection, the shape-dependent model is presented. Now, we discuss another type of growth mechanism, which is independent of the shape of the nanoparticles. The simplest case is a constant kinetic factor along the preferred growth direction, say x. With this assumption, we obtain the kinetic term as $\boldsymbol{F}^{\mathrm{k}} = (1,0,0)^{\mathrm{T}}$. To be clarified with the parameter γ in Eq. (6), γ in Eq. (3) is replaced by α. Then equation (3) is deduced to

$$\boldsymbol{P} = (1-\alpha)\frac{\boldsymbol{S}}{S_{\mathrm{a}}} + \alpha \begin{bmatrix} 1 \\ 0 \\ 0 \end{bmatrix}. \tag{7}$$

It is known that, at the initial stage of the growth, since $P_x > P_y$, the inhomogeneous growth along the x direction takes place and therefore the nanoparticles gradually elongate along the x-direction and deviate from cubes. Since the symmetry is broken along the x-axis, it is predictable that $l_x > l_y \sim l_z$. Defining that $r_0 \equiv l_x/l_y \sim l_x/l_z$, the following equations are obtained from Eq. (7):

$$P_x = \frac{1+2r_0\alpha}{1+2r_0}, \tag{8a}$$

$$P_y \sim P_z = \frac{(1-\alpha)\,r_0}{1+2r_0}. \tag{8b}$$

It is known that $l_i \propto v_i \propto P_i$, where v_i is the growth rate along the i-direction. Therefore, the equation $l_x/l_y = P_x/P_y = r_0$

holds. Then by substituting Eq. (8) into this equation, we can deduce the relationship between r_0 and α as

$$r_0 = \frac{\alpha + \sqrt{\alpha^2 - \alpha + 1}}{1 - \alpha}. \tag{9}$$

This means that when l_x is large enough, the growth reaches a stable stage, when the ratio between P_x and P_y keeps a constant. What should be emphasized is that equation (6) holds only for large cuboid nanoparticles ($l_{x,y,z} \gg 1$).

3. Results and discussion

Following the models established in Section 2, we perform a Monte Carlo simulation for the growth of the cuboid nanoparticles. In the simulation, we carry out a growth process from a $5 \times 5 \times 5$ size cube. In each step, a random number ranged from 0 to 1 is sampled by Eqs. (4), (6), or (7), respectively, for the three models. A new layer is added according to the face when the random number falls into the probability range of it. This process of the layer growth continues until a certain size of the cuboid nanoparticle is reached. The simulation is repeated to obtain a large population of the cuboid-shaped nanoparticles. Three values are introduced here to describe the deviated degree of the particles from a cube. One is the aspect ratio r, which is the ratio between the longest and the shortest sides and has been defined before. Another one is introduced to characterize the difference between all the three sides of a cuboid and is written as

$$D = \frac{(l_x - l_y)^2 + (l_y - l_z)^2 + (l_z - l_x)^2}{l_x^2 + l_y^2 + l_z^2}. \tag{10}$$

Furthermore, we can also define

$$P'_r = \sum_{r \geq r'} P(r), \tag{11}$$

which is the possibility that the aspect ratio r is larger than value r'. Here $P(r)$ is the distribution function of r. The sum is over all the nanoparticle configurations obtained. Now, based on the large numbers of cuboid nanoparticles obtained through our simulation, the distributions of D and r can be obtained and P'_r can also be calculated. The average atom number N over all the products can also be obtained and is denoted as $\bar{N}$. For typical experimental batches, there are 1 to 1000 million nanoparticles generated. To make the simulation result comfortably represent the real case, a comparable number of repetitions should be performed. Balancing the computation time, we conduct at least 5×10^5 repetitions in each case. The statistical errors for D, r, P'_r, and $\bar{N}$ are all smaller than 0.1%.

To give a clear impression of the size of the obtained cube-shaped nanoparticles, we calculate the atom number of the platinum (Pt) cubes with the side length l. The results are shown in Table 1.

Table 1. Atom numbers of Pt cube-shaped nanoparticles with side length l.

l/nm	5	10	20	50
$\bar{N}$	8.25×10^3	6.60×10^4	5.28×10^5	8.25×10^6

3.1. Growth of cuboid nanoparticle due to thermodynamics

We further study the shape distribution of the cuboid nanoparticles when only the thermodynamic factor is considered and the results are shown in Fig. 2. The distributions of D and r for four cases with different average atom numbers $\bar{N}$ are given in Figs. 2(a) and 2(b), respectively. Each dot in the figure stands for one configuration of the cuboid nanoparticles. The normalization of the distributions of D and r is satisfied,

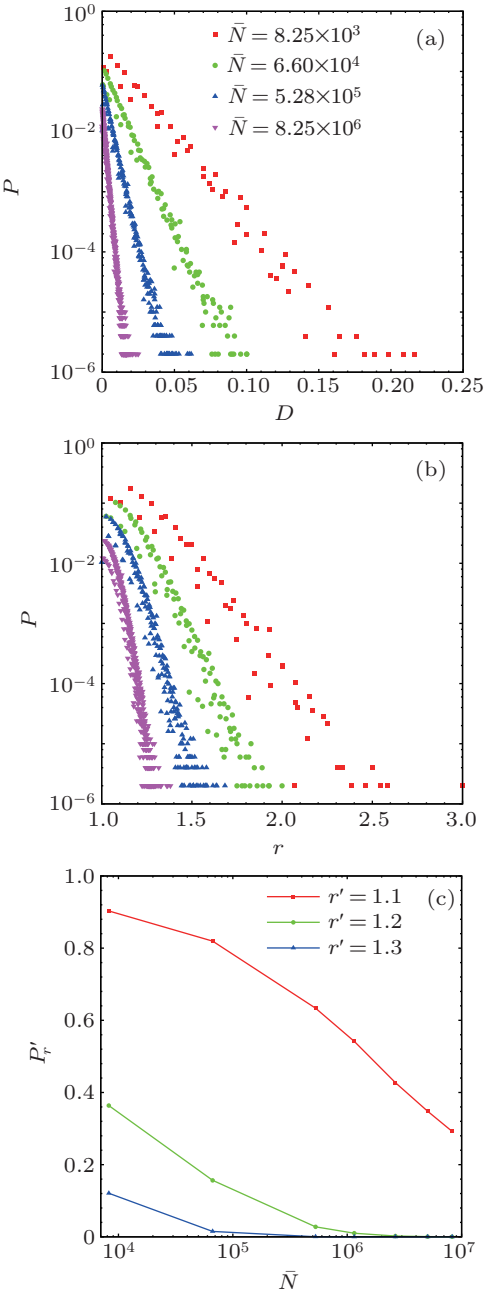


Fig. 2. The distributions of P with (a) D and (b) r for the cases with different average atom numbers $\bar{N}$. (c) P'_r for $r' = 1.1$, 1.2, 1.3 as functions of average atom number $\bar{N}$.

which means $\sum P = 1$, where the sum is over all nanoparticle configurations obtained. Figures 2(a) and 2(b) show that the possibilities of D and r for the small $\bar{N}$ (8.25×10^3) case are always larger than those for larger atom numbers cases. When $\bar{N}$ is 8.25×10^3, each side of the particles has only about 20 atoms. This means that each face addition would change the aspect ratio by about $1/20$, which is a strong influence and results in a large deviation. However, with increasing $\bar{N}$, the distributions of D and r trend toward 0 and 1, respectively. It is implied that the difference between three sides becomes smaller with the increasing size of the cuboid nanoparticles. The addition of a new face will almost not affect the aspect ratio when the side length is much larger than the atom diameter. Figure 2(c) shows that $P_{1.1}$, $P_{1.2}$, and $P_{1.3}$ all decrease with increasing $\bar{N}$. For example, when $\bar{N} \sim 8.25 \times 10^3$, $P_{1.2}$ is about 0.29. When $\bar{N}$ is increased to 10^6, $P_{1.2}$ is almost zero. These results indicate that the possibility is large that the nanoparticle shape deviates from the cube only at the initial stage of the growth. It is consistent with the homogeneous assumption of the thermodynamic factor (see Eq. (4)) that the asymmetrical growth will gradually vanish with the increase of the particle size. When the particle size is smaller than 10 nm, cuboid particles are more likely to be visible, and the aspect ratios of them are usually smaller than 1.5, which is consistent with the observation in almost every experimental attempt for nanocubes.

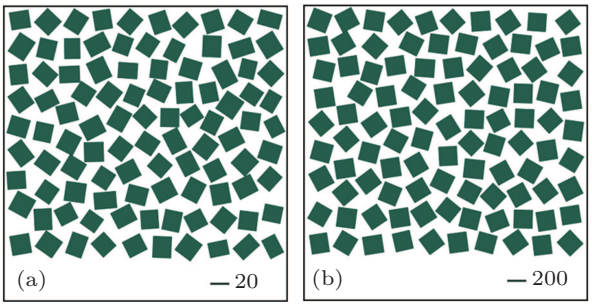


Fig. 3. Schematic images of the grown cuboid nanoparticles affected only by the thermodynamic factor for (a) $\bar{N} \sim 8.25 \times 10^3$ and (b) $\bar{N} \sim 8.25 \times 10^6$.

Schematic images are presented for comparing our simulation to the experiments. In the experiments, one usually takes SEM or TEM images after the formation of the cuboid nanoparticles, which always lay on the base. It always looks like a batch of squares and rectangles spread in a plane. 100 simulated nanoparticles are picked randomly from our simulation, and are laid on a random face to form the schematic images shown in Fig. 3. In consideration of the small r, it is assumed that the face which we can see is selected from all the six faces randomly with equal possibility. Figure 3(a) shows that there is a considerable portion of cuboid nanoparticles accompanying the cube-shaped nanoparticles when the size of the nanoparticle is small. The aspect ratios of some of the cuboid nanoparticles are even larger than 1.2. When the size is increased (Fig. 3(b)), the nanoparticles become much more regular and their shape ratios are almost 1. Therefore, in an experimental system, if the thermodynamic factor is dominant, when the particle size is small, the product contains cuboid and cube-shaped nanoparticles together. However, the final product tends to be all cubes.

3.2. Growth dominated by the model with both thermodynamic and shape-dependent kinetic factors

We now turn to study the influence of the kinetic together with the thermodynamic factor on the shape of the cuboid nanoparticles. First, the growth process governed by both thermodynamic factor and shape-dependent kinetic factor (see Eq. (6)) is simulated. We consider two conditions of $\gamma = 0.5$ and 1 and the corresponding results are shown in Figs. 4(a), 4(b) and 4(c), 4(d), respectively. In each figure, four cases for different average atom numbers are shown. Figures 4(a) and 4(b) show that when $\gamma = 0.5$, the distributions of D and r are gradually asymptotic to 0 and 1, respectively, with increasing $\bar{N}$. The nanoparticle tends to be cube-shaped when its size is large enough. This feature is similar to the case with only the thermodynamic factor existing (see Figs. 2(a) and 2(b)). This result implies that at least up to $\gamma = 0.5$ (from 0), the thermodynamic term is still dominant. However, when γ is increased to 1, the results are different. In Figs. 4(c) and 4(d), D and r deviate gradually away from 0 and 1, respectively, with increasing $\bar{N}$. This comes from the fact that more and more nanoparticles take cuboid shape with larger possible aspect ratio. We have mentioned that when $\gamma = 1$, the growth is dominated only by the kinetic factor (see Eq. (7)). Once the asymmetrical growth takes place along one direction, the kinetic term gives a positive feedback mechanism and continues to lengthen the nanoparticle along this direction.

It is interesting that the growth trends for $\gamma = 0.5$ and 1 are opposite, which reflects the different properties of the thermodynamic and kinetic factors. In order to address the two different trends more clearly, $\langle r \rangle$ is introduced, which stands for the average value of aspect ratio r. $\langle r \rangle$ can be calculated based on the distribution of r. The result is shown in Fig. 5(a). For $\gamma = 0$, when only the thermodynamic factor affects the growth, $\langle r \rangle$ decreases with $\bar{N}$ and is asymptotic to 1. On the contrary, $\langle r \rangle$ increases with $\bar{N}$ for $\gamma = 1$ when the kinetic factor dominates the growth. For $0 < \gamma < 1$, both of the thermodynamic and kinetic factors exist. $\langle r \rangle$ decreases with $\bar{N}$ when γ is relatively small (see the curves for $\gamma = 0.75$ and 0.9). Then it is interesting to find that for $\gamma = 0.95$ and 0.97, $\langle r \rangle$ first increases and then decreases with $\bar{N}$. This result reflects the competition of the thermodynamic and kinetic factors. When γ is relatively large (see the curve for $\gamma = 0.99$), $\langle r \rangle$ increases with $\bar{N}$. To further understand which factor dominates with

different γ, $\langle r\rangle$ values have been calculated as a function of γ (Fig. 5(b)) for three different $\bar{N}$. Three curves cross at different γ values. Three intersection points are: I at about $\gamma = 0.93$ for $\bar{N} = 8.25\times10^3$ and 6.60×10^4 cases; II at about $\gamma = 0.95$ for $\bar{N} = 8.25\times10^3$ and 8.25×10^6 cases; III at about $\gamma = 0.96$ for $\bar{N} = 8.25\times10^3$ and 8.25×10^6 cases. When γ is smaller than all these three intersection points, $\langle r\rangle$ decreases with increasing $\bar{N}$. On the contrary, when $\langle r\rangle$ is larger than these interaction points, $\langle r\rangle$ increases with the increase of $\bar{N}$. When $\langle r\rangle$ is at the other range, $\langle r\rangle$ first increases and then decreases with increasing $\bar{N}$.

To help us understand the numerical result, the schematic images are generated for $\gamma = 1$ at different $\bar{N}$ in Fig. 6. Since long cuboids lay on their sides in experiments, when the aspect ratio is near to 1, we can select one face from the six faces randomly with equal possibility. However, when r is too large, the cuboid nanoparticles become nanorods and are more likely

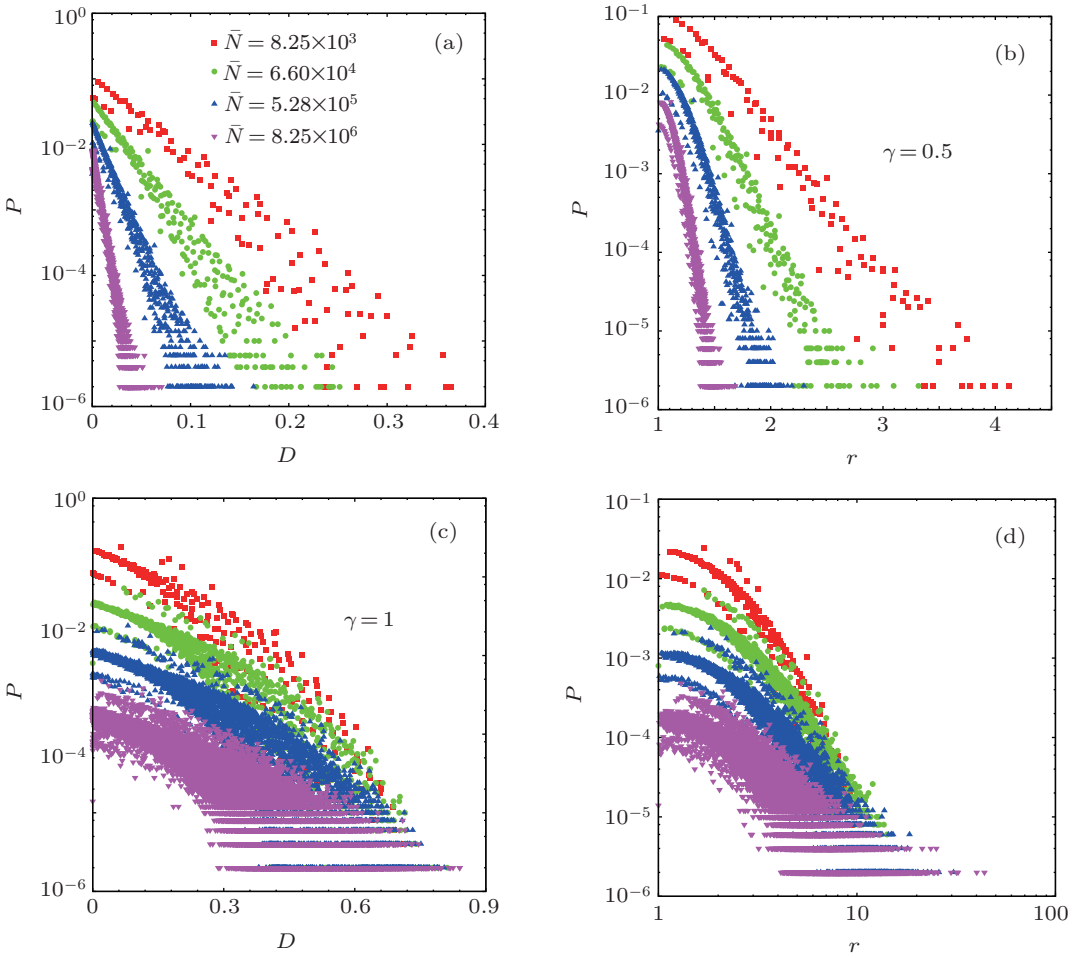


Fig. 4. The distributions of P with D ((a) and (c)) and r ((b) and (d)) for $\gamma = 0.5$ ((a) and (b)) and 1 ((c) and (d)). In each figure, four cases for different average atom numbers $\bar{N}$ are shown.

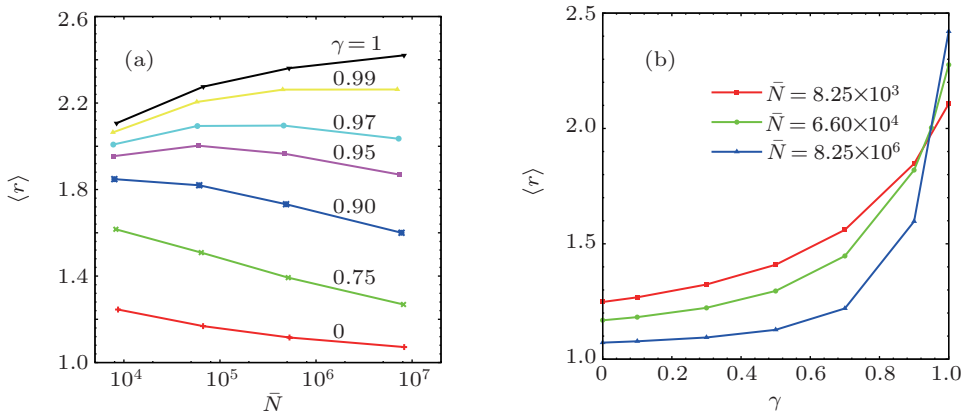


Fig. 5. The average aspect ratio $\langle r\rangle$ as a function of (a) $\bar{N}$ for $\gamma = 0$, 0.75, 0.9, 0.95, 0.97, 0.99, 1, and (b) γ for $\bar{N} = 8.25\times10^3$, 6.60×10^4, 8.25×10^6.

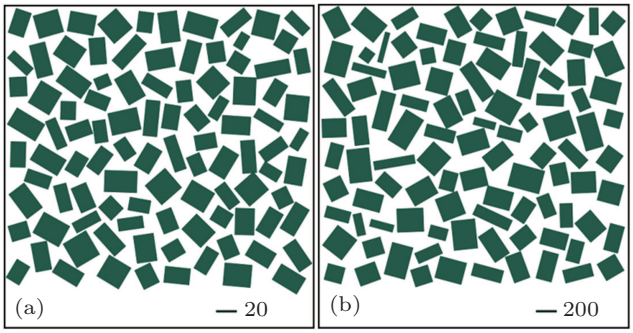


Fig. 6. Schematic images of the grown cuboid nanoparticles for (a) $\bar{N} = 8.25 \times 10^3$ and (b) $\bar{N} = 8.25 \times 10^6$. In the simulation, $\gamma = 1$.

likely to lie down rather than standing on the tip. Therefore, it is assumed that the face seen is selected from four larger faces with equal possibility. Figure 6(a) shows that different shaped nanoparticles can be obtained when $\bar{N}$ is small. Some are cubes and some others are cuboids. Particularly, the aspect ratios of some nanoparticles are even greater than 2. Figure 6(b) shows that the shapes of the nanoparticles are more irregular when $\bar{N}$ is large. Some particles keep cube-shaped, whereas some others elongate and even become nanorods. These two figures reflect the effect of the kinetic term. If the experimental results are similar to these two figures, which obtain cube-shaped, cuboid-shaped, and rod-shaped nanoparticles, there must be a shape-dependent kinetic factor which provides an inhomogeneous growth mechanism. It is interesting to find that our simulation results in Fig. 6(b) are similar to the TEM images of Pd nanostructures obtained in the experiment by Xiong.[23] In that experiment, the localized-oxidative-etch is thought to be the mechanism which induces the inhomogeneous growth along one direction.

3.3. Growth dominated by the model with both thermodynamic and shape-independent kinetic factors

We then discuss the growth of the cuboid nanoparticles following the model with both thermodynamic and shape-independent kinetic factors. Two cases for small and large α are considered and the simulation results are shown in Fig. 7. In each figure, three conditions with different numbers of atoms are shown. When α is small (0.1 in Figs. 7(a) and 7(b)), it is interesting to see that with the increasing atom number $\bar{N}$, the distributions of D and r both become packets gradually. This implies that the final shape of the nanoparticles is a cuboid and the aspect ratio is concentrated around a certain value. It is also seen that the full width at half maximum (FWHM) of the packet decreases with the increase of $\bar{N}$. This implies that with increased size of the nanoparticles, the shape of the grown products becomes more and more uniform.

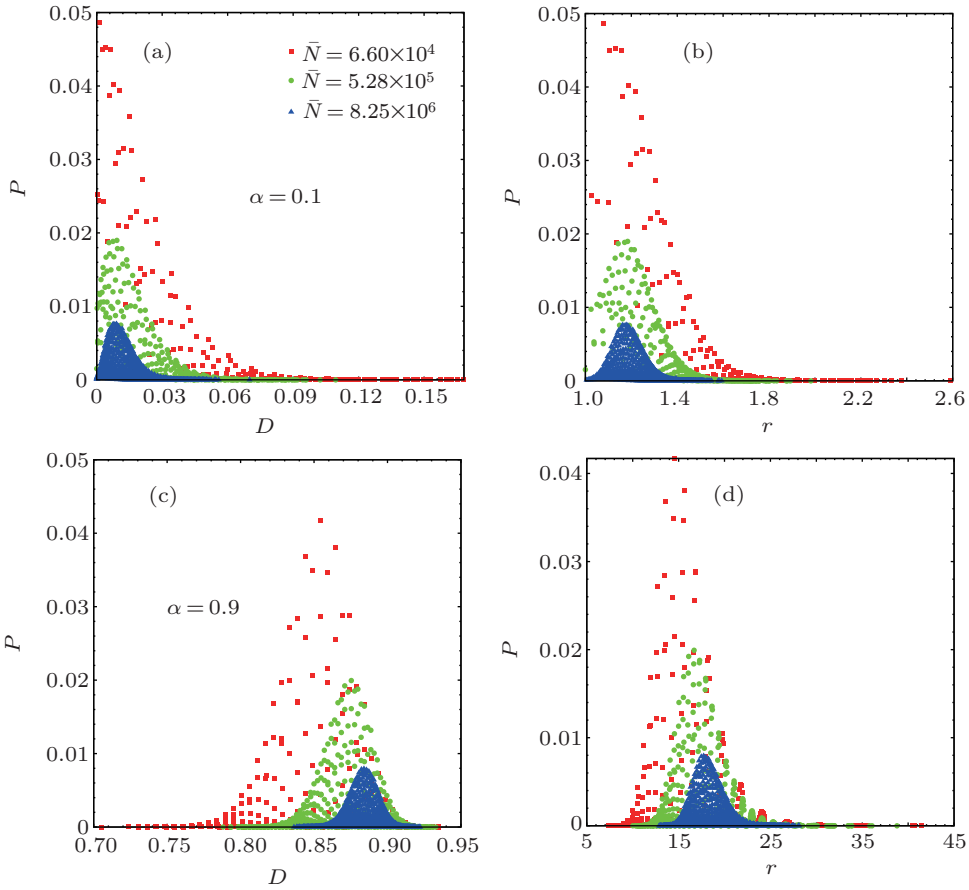


Fig. 7. The distributions of P with D ((a) and (c)) and r ((b) and (d)) for $\alpha = 0.1$ ((a) and (b)) and $\alpha = 0.9$ ((c) and (d)). In each figure, three cases for different average atom numbers $\bar{N}$ are shown.

The aspect ratios of all the cuboid nanoparticles are asymptotic to r_0 if the average size is large enough. This feature has been explained analytically in Subsection 2.3. In the early stage of the growth, due to the kinetic term along the x direction, P_x is larger than P_y and P_z and thus growth along the x direction is the fastest. When the growth reaches the stable growth stage, the nanoparticle continues to elongate and at the same time it thickens, while r keeps a constant. Therefore, the distributions of D and r are packets. Figures 7(c) and 7(d) show the results when α is increased to 0.9. In this condition, it is obvious to find that the packet centers of D and r become larger compared to those of the corresponding cases with $\alpha = 0.1$ in Figs. 7(a) and 7(b). For example, for a larger size nanoparticle ($\bar{N} = 8.25 \times 10^6$), the most probable r is as large as 18.1. What should be emphasized is that $r_0 \to +\infty$ when $\alpha = 1$ according to Eq. (9). This means that $P_x = 1$ and $P_y = P_z = 0$. The product nanostructure will be a nanowire with the y, z dimensions of the original seeds.

Then the average values of r for different α values based on the simulation results are calculated and shown in Fig. 8. Only $\langle r \rangle$ for large $\bar{N}$ are presented since the theoretical r_0 is reached when $\bar{N} \to +\infty$. At this stage, $\langle r \rangle \approx r_0$ when the calculation is precise enough. It is seen that $\langle r \rangle$ increases with α, which means that the stronger the kinetic factor is, the longer the cuboid nanoparticles are. At the same time, the analytical results by Eq. (9) are also shown. The simulation result matches the analytical values very well.

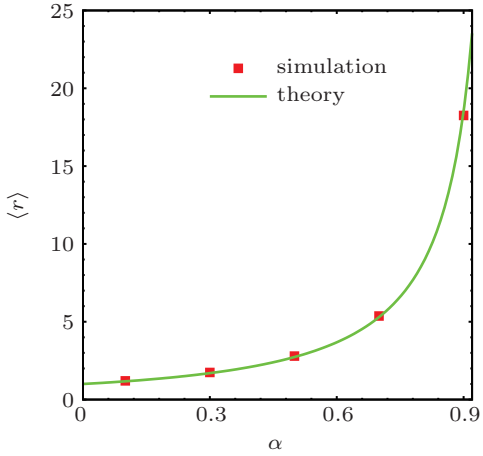


Fig. 8. (color online) Average value of the aspect ratio, $\langle r \rangle$, as a function of the kinetic term α. Both the simulation and the analytical results are shown.

To present our simulation results more clearly, we generate schematic images based on the simulation data in Fig. 9. Similar to Fig. 6, 100 nanoparticles are chosen randomly based on the shape distribution obtained from the simulation. For small α (0.1 in Fig. 9(a)), although the kinetic factor is included, the growth products still remain cuboid nanoparticles accompanying with cube-shape nanoparticles and the aspect ratio r is close to 1. In contrast, when α is increased to 0.9 (Fig. 9(b)), the morphology of the growth products changes a lot. The aspect ratio is very large (~ 18.1) and thus the nanoparticles become nanorods. This result indicates that the kinetic factor is more dominant to the final shape. Experimentally, if rod-shaped products with similar aspect ratio are found, there should be a kinetic mechanism which is independent of the shape of the nanoparticles.

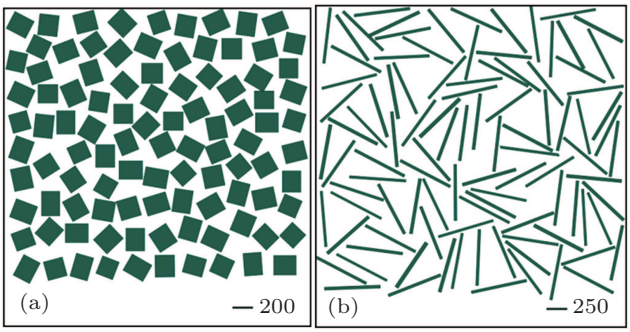


Fig. 9. Schematic images of the grown cuboid nanoparticles for (a) $\alpha = 0.1$ and (b) 0.9. In the simulation, $\bar{N} = 8.25 \times 10^3$.

4. Conclusion and perspectives

The effects of the thermodynamic and kinetic factors on the asymmetrical growth of the cube-shaped nanoparticles have been investigated by the Monte Carlo method. Based on different types of growth processes in experiments, we simplified the universal model into three cases with specified physical concepts. They are a) thermodynamic factor only model; b) thermodynamic with shape-dependent kinetic factor model; and c) thermodynamic with shape-independent kinetic factor model. For the first growth model, the possibility that the nanoparticles deviate from the cube-shape is large (when $\bar{N} \sim 10^3$, $p_{1,2} \sim 0.3$) at the early stage of the growth, when the size of the nanoparticles is small. However, when the size of the nanoparticles is large, due to the homogeneous property of the thermodynamic factor, the possibility of deviating from cubes is fairly low. This result can explain why there is a considerable portion of cuboid nanoparticles accompanying the cube-shaped nanoparticles obtained in the experiments when the size of the nanoparticles is small, no matter what the materials and experimental conditions are. For the model with both thermodynamic and shape-dependent kinetic factors, the thermodynamic factor is dominant for a wide range ($0 < \gamma < 0.93$), for which case the nanoparticle tends to be a cube when its size is large enough. When $0.96 < \gamma < 1$, the kinetic factor plays a leading role and makes the nanoparticle elongated. The final products have different appearances, including the cube-shaped, cuboid, and rod-shaped nanoparticles. This result explains the experiments in which nonuniform shaped products are obtained. Finally, a model with both thermodynamic and shape independent kinetic factors were analyzed. The kinetic factor accelerates the growth along one direction until

the growth process reaches a stable stage where r is a constant. This result explains the type of experiments in which uniform nanorods are obtained. Our simulation based on three simplified phenomenological models successfully represents three major types of known nanoparticle products in experimental works. This theoretical work benefits the understanding of the cause and manner of the asymmetrical growth of nanoparticles and could be useful for guiding the shape control of metallic nanostructures.

References

[1] Xia Y, Xiong Y, Lim B and Skrabalak S E 2009 *Angewandte Chemie-International Edition* **48** 60

[2] Tao A R, Habas S and Yang P 2008 *Small* **4** 310

[3] Kvitek O, Siegel J, Hnatowicz V and Svorcik V 2013 *Journal of Nanomaterials* **2013** 15

[4] Xiao J and Qi L 2011 *Nanoscale* **3** 1383

[5] Seo D, Park J C and Song H 2006 *J. Am. Chem. Soc.* **128** 14863

[6] Murphy C J, Gole A M, Hunyadi S E and Orendorff C J 2006 *Inorganic Chemistry* **45** 7544

[7] Chen J, Wiley B J and Xia Y 2007 *Langmuir* **23** 4120

[8] Shen X S, Wang G Z, Hong X, Xie X, Zhu W and Li D P 2009 *J. Am. Chem. Soc.* **131** 10812

[9] Pastoriza-Santos I and Liz-Marzan L M 2008 *Journal of Materials Chemistry* **18** 1724

[10] Halder A and Ravishankar N 2007 *Adv. Mater.* **19** 1854

[11] Zhang Q, Liu S J and Yu S H 2009 *Journal of Materials Chemistry* **19** 191

[12] Porter D A and Easterling K E 1981 *Phase Transformations in Metals and Alloys* (New York: Chapman and Hall)

[13] Yu D and Yam V W W 2004 *J. Am. Chem. Soc.* **126** 13200

[14] Niu W, Li Z Y, Shi L, Liu X, Li H, Han S, Chen J and Xu G 2008 *Crystal Growth & Design* **8** 4440

[15] Lee H, Habas S E, Kweskin S, Butcher D, Somorjai G A and Yang P 2006 *Angewandte Chemie* **45** 7824

[16] Wang C, Daimon H, Lee Y, Kim J and Sun S 2007 *J. Am. Chem. Soc.* **129** 6974

[17] Xu D, Liu Z, Yang H, Liu Q, Zhang J, Fang J, Zou S and Sun K 2009 *Angewandte Chemie-International Edition* **48** 4217

[18] Huang X, Zhang H, Guo C, Zhou Z and Zheng N 2009 *Angewandte Chemie-International Edition* **48** 4808

[19] Wang S B, Min Y L and Yu S H 2007 *Journal of Physical Chemistry C* **111** 3551

[20] Yang S and Gao L 2006 *J. Am. Chem. Soc.* **128** 9330

[21] Sun Y, Zhang L, Zhou H, Zhu Y, Sutter E, Ji Y, Rafailovich M H and Sokolov J C 2007 *Chemistry of Materials* **19** 2065

[22] Pérz-Juste J, Liz-Marzán L M, Carnie S, Chan D Y C and Mulvaney P 2004 *Advanced Functional Materials* **14** 571

[23] Xiong Y, Cai H, Wiley B J, Wang J, Kim M J and Xia Y 2007 *J. Am. Chem. Soc.* **129** 3665

[24] Viswanath B, Kundu P, HaIder A and Ravishankar N 2009 *Journal of Physical Chemistry C* **113** 16866

[25] Kossel W 1927 *Nachr. Gesellschaft Wiss Gottingen* **143**

[26] Stranski I 1927 *Jahrb. Univ. Sofia (Phys. Math. Fac.)* **2** 297

[27] Stranski I Z 1928 *Phys. Chem. A* **136** 259